

## Article

# Screening, Characterization and Probiotic Properties of Selenium-Enriched Lactic Acid Bacteria

Lixia Zan <sup>1,2</sup>, Zhe Chen <sup>2</sup>, Ben Zhang <sup>2</sup>, Xiangyu Zou <sup>2</sup>, Afeng Lan <sup>2</sup>, Wenyi Zhang <sup>2</sup>, Yahong Yuan <sup>1,3</sup> and Tianli Yue <sup>1,3,\*</sup>

<sup>1</sup> College of Food Science and Engineering, Northwest A&F University, Xianyang 712100, China; zanlx@126.com (L.Z.); 13891630597@163.com (Y.Y.)

<sup>2</sup> College of Biological Sciences and Engineering, Shaanxi Province Key Laboratory of Bio-Resources, QinLing-Bashan Mountains Bioresources Comprehensive Development C. I. C., Qinba State Key Laboratory of Biological Resources and Ecological Environment, Tea Planting and Processing Research Institute, Shaanxi University of Technology, Hanzhong 723000, China; 18391312429@163.com (Z.C.); 15667293341@163.com (B.Z.); 800403@163.com (X.Z.); lanafeng@snut.edu.cn (A.L.); 13991557061@163.com (W.Z.)

<sup>3</sup> College of Food Science and Technology, Northwest University, Xi'an 710069, China

\* Correspondence: yuetl305@nwsuaf.edu.cn; Tel.: +86-13572858832

**Abstract:** Considerable progress has been achieved in the bioaccumulation and transformation of selenium (Se)-enriched lactic acid bacteria (LAB). However, research on the effects of Se on the structure and probiotic potential of LAB is relatively limited. In this study, six industrial LAB strains, including *Lactobacillus plantarum* 21,805, *Lactobacillus paracasei* 20,241, *Lactobacillus fermentum* 21,828, *Lactobacillus casei* 23,185, *Lactobacillus acidophilus* 6064, and *Lactobacillus plantarum* 6076, were cultured in De Man, Rogosa, and Sharpe (MRS) medium containing Se for three generations. High-Se LAB was screened based on bacterial biomass, viable bacterial count, and Se content. Their structural characteristics were analyzed using scanning electron microscopy (SEM), Fourier-transform infrared spectroscopy (FTIR), and X-ray diffraction (XRD). The results indicated that LAB growth was influenced by the Se environment, with high Se (20 µg/mL) inhibiting it. At a Se concentration of 10 µg/mL, LAB maintained integrity and exhibited a high Se enrichment ability, with a Se enrichment of  $4.88 \pm 0.39$  mg/g. The intracellular Se existed in an amorphous or non-crystalline form. Furthermore, Se-enriched LAB exhibited enhanced probiotic properties, including tolerance to simulated gastrointestinal fluids, acid resistance, bile salt resistance, and hydrophobicity. Therefore, Se-enriched LAB are expected to develop new functional foods or dietary supplements for human and animal consumption.

**Keywords:** lactic acid bacteria; *Lactobacillus plantarum*; structural characterization; probiotic properties



**Citation:** Zan, L.; Chen, Z.; Zhang, B.; Zou, X.; Lan, A.; Zhang, W.; Yuan, Y.; Yue, T. Screening, Characterization and Probiotic Properties of Selenium-Enriched Lactic Acid Bacteria. *Fermentation* **2024**, *10*, 39. <https://doi.org/10.3390/fermentation10010039>

Academic Editor: Mutamed Ayyash

Received: 11 October 2023

Revised: 29 November 2023

Accepted: 6 December 2023

Published: 3 January 2024



**Copyright:** © 2024 by the authors. Licensee MDPI, Basel, Switzerland. This article is an open access article distributed under the terms and conditions of the Creative Commons Attribution (CC BY) license (<https://creativecommons.org/licenses/by/4.0/>).

## 1. Introduction

Se is recognized as an essential trace element for human health [1]. It plays a crucial role in numerous physiological functions, including but not limited to combating oxidative stress, regulating growth, reducing pregnancy complications, enhancing fertility, and antiviral activity [2]. The World Health Organization (WHO) has recommended a daily intake of 55 µg of Se for maintaining human health [3]. However, Se-deficient areas are widespread across the globe, and currently around 0.5–1.0 billion people are at risk of Se deficiency [4]. Inadequate Se intake, particularly below 20 µg/d in adults, has been linked to various health issues such as Keshan disease, Kashin–Beck disease, hypothyroidism, cardiovascular diseases, weakened immune systems, male infertility, memory loss, and an increased risk of various cancers [5].

Probiotics are composed of a diverse array of microorganisms, including bacteria such as *Lactobacillus* and *Bifidobacterium*, as well as yeast such as *Saccharomyces boulardii* [6,7].

These bacteria ferment carbohydrates, leading to the production of lactic acid, which is beneficial in maintaining a healthy balance in the gut microbiota by inhibiting the growth of harmful bacteria [8]. In the industrial setting, probiotics can be mass-produced in large bio-reactors to meet the cell requirements for functional food production [9]. The industrial application of probiotics has expanded to various fields, including food and beverage production, pharmaceuticals, and agriculture.

As a prominent group of common probiotics, LAB naturally exist in the human intestine and various food sources, with traditional fermented foods serving as a good source to obtain these bacteria, including yogurt, kimchi, sauerkraut, kefir, and sourdough bread [10]. LAB play a crucial role in maintaining the balance of intestinal microecology, immune regulation, anti-cancer, antibacterial, and antiviral activities [11,12]. They also contribute to improved digestion of lactose and micronutrients, reduction in antibiotic-associated diarrhea, and mitigation of the risk of vaginal infections [13].

In the context of bioconversion, Se-enriched LAB have demonstrated the capability to convert inorganic Se into organic selenides [14]. Research has indicated that Se-enriched LAB not only aid in meeting the Se requirements of populations with Se deficiency but also play a significant role in disease prevention, enhancement of immune function, and protection of gastrointestinal health [15].

In recent years, significant advancements have been achieved in research on the bioaccumulation and biotransformation capabilities of Se-enriched LAB. However, research focusing on the structure and probiotic potential of these Se-enriched LAB remains relatively limited [16]. This study investigated the effect of Se concentration on the growth and enrichment of LAB, and evaluated the probiotic characteristics of Se-enriched LAB. The aim is to provide a scientific basis for the development of Se-enriched LAB products by gaining a deeper understanding of the mechanisms of LAB Se enrichment and adaptation.

## 2. Materials and Methods

### 2.1. Strains and Reagents

*L. plantarum* 21,805, *L. paracasei* 20,241, *L. fermentum* 21,828, *L. casei* 23,185, *L. acidophilus* 6064, and *L. plantarum* 6076 were purchased from China Center of Industrial Culture Collection (CICC) (China).

Se<sup>2+</sup> single-element standard solution (214021-3) was acquired from the National Nonferrous Metals and Electronic Materials Analysis and Testing Center (NMT) (Beijing, China). All other reagents were of analytical grade and were purchased from Beijing Aoboxing Biotechnology Co., Ltd. (Beijing, China).

### 2.2. Strain Activation and Expansion Culture

All strains were cultured in MRS medium at 37 °C for three generations, with each generation being of 24 h. During the culture period, the absorbance at 600 nm measured using (U-3900, Hitachi, Tokyo, Japan) was recorded every 2 h for 24 h, and the growth curve at 600 nm was plotted. Each experiment was repeated three times.

### 2.3. Se-Enriched Bacterial Cultivation

Each strain was individually cultured in MRS medium with Se concentrations of 0, 5, 10, 20, and 40 µg/mL at 37 °C for three generations, with each generation lasting 24 h. All experiments were conducted with cultures of passage 3. The absorbance at 600 nm was measured every 3 h, and the number of viable bacteria was determined using the plate coating method to calculate the colony-forming unit (CFU). At the end of the incubation, the bacterial solution cultured at each Se concentration was centrifuged at 5000 rpm for 15 min (H1850R, Xiangyi, Neijiang, China), washed three times with phosphate-buffered saline (PBS), and the precipitated bacterial biomass was freeze-dried.

#### 2.4. Se Content Determination

The Se content in the freeze-dried biomass of each strain was determined using a hydride generation atomic fluorescence spectrometer (AFS230E, Haiguang, Beijing, China) following a previously described method [17]. Argon was utilized as the carrier gas, 5% HCl as the carrier flow, and a 2% NaBH<sub>4</sub> solution as the reducing agent. The instrument conditions were set as follows: a negative high voltage of 300, a reading time of 15 s, a delay time of 3 s, and each sample was analyzed in triplicate.

#### 2.5. Strain Identification by 16S rRNA Sequencing

Genomic DNA was extracted using Tiangen Bacterial Genomic DNA Extraction Kits (Tiangen, Beijing, China). The DNA was then amplified by PCR using the universal primer pair 27F (5′-AGAGTTTGATCCTCGCTCAG-3′) and 1492R (5′-GGTTACCTTGTTACGACTT-3′), targeting the bacterial 16S rRNA gene. The PCR reaction system (50 µL) comprised 2 × Taq PCR Master Mix (With Dye) 25 µL, template DNA 2 µL, upstream and downstream primers (10 µmol/L) 2 µL each, and ddH<sub>2</sub>O 19 µL. The PCR was initiated at 94 °C for 5 min, followed by 36 cycles at 92 °C for 30 s, 56 °C for 30 s, and 72 °C for 90 s, and concluded with a final extension step at 72 °C for 10 min. Subsequently, 2 µL of the PCR products was subjected to 1.0% agarose gel electrophoresis and visualized using a UV gel imaging system. The resulting PCR amplicons were sent to Sangon Bioengineering (Shanghai, China) Co., LTD for sequencing. Sequence similarity analysis was performed using the BLAST program of NCBI to identify closely related sequences and determine the taxonomic classification of the bacteria. Sequences with a similarity of 97% or higher were considered as potential new bacterial species, while those with less than 97% similarity were regarded as potential new species [18]. Pairwise distances were computed using MEGA 11.0 software to calculate genetic distances, and the neighbor-joining method was employed to construct phylogenetic trees based on the 16S rRNA gene sequences obtained from sequencing. Bootstrap analysis was performed 1000 times to assess the confidence intervals of the evolutionary tree topology.

#### 2.6. Characterization Methods

##### 2.6.1. SEM Analysis

The SEM assay was conducted in accordance with a previously described method [19]. Freeze-dried samples of LAB were gold-coated and examined for surface morphology using a scanning electron microscope (Verios 460, Thermo Fisher, Waltham, MA, USA) with an accelerating voltage of 10 kV.

##### 2.6.2. FT-IR Analysis

The FT-IR assay was carried out following a previously described method [20]. A Fourier transform infrared spectrometer (NICOLET IS50, Thermo Scientific, Waltham, MA, USA) was employed for infrared spectrum analysis within the range of 4000–500 cm<sup>-1</sup>.

##### 2.6.3. XRD Analysis

The lyophilized bacteria powder was compressed into a glass groove, and an X-ray diffractometer (D8 Advance, Bruker, Germany) was used with a scanning angle range of 2θ (5°–70°) at room temperature, an operating voltage of 40 kV, a current of 40 mA, and a copper target X-ray source (Cu Kα, λ = 0.15406 nm). The scanning speed was set at 12°/min [20].

#### 2.7. Probiotic Properties Assessment

##### 2.7.1. Evaluation of Tolerance to Artificial Gastric and Intestinal Fluids

In accordance with the approach outlined by Shu et al. [21], a 1 mL bacterial suspension of each strain was combined with 9 mL of artificial gastric fluid (comprising 0.2 g sodium chloride and 1 g pepsin dissolved in 100 mL HCl solution at pH 2.0) and incubated statically at 37 °C. The treatment solution was sampled at 0, 30, 60, 90, and 120 min intervals to

assess the number of viable bacteria. Additionally, 1 mL of artificial gastric fluid containing bacteria was mixed with 9 mL of artificial intestinal fluid (comprising 0.68 g potassium dihydrogen phosphate and 1.0 g trypsin dissolved in 100 mL of distilled water, with pH adjusted to 7 using NaOH solution). The mixture was incubated at 37 °C for 150, 180, 210, and 240 min, and the viable bacterial count was determined to calculate the survival rate using the following formula:

$$\text{Survival Rate (\%)} = (A_S/A_0) \times 100\%$$

where  $A_S$  represents the survival count of the strain treated in simulated gastric or intestinal fluid, and  $A_0$  represents the initial survival count of the strain.

### 2.7.2. Assessment of Acid Tolerance

The acid tolerance of the strains was determined following the method of Taj et al. [22] with slight modifications. The pH was adjusted by adding 0.1 mol/L HCl. Each strain was inoculated in MRS medium (pH 2, 3, 7) and statically incubated at 37 °C for 5 h. The OD<sub>600</sub> value was measured, and the acid tolerance was calculated using the following formula:

$$\text{Acid Tolerance (\%)} = 1 - (A_n - A_a)/A_n \times 100\%$$

where  $A_n$  represents the value of OD<sub>600</sub> at pH 7, and  $A_a$  represents the value of OD<sub>600</sub> at pH 2 or pH 3.

### 2.7.3. Determination of Bile Salt Tolerance

The tolerance of each strain to bile salts was determined following Kaur's method [23]. Each strain was inoculated at 1% in MRS medium with different concentrations of bile salts (0%, 0.3%, 0.5%). After incubation at 37 °C for 6 h, the OD<sub>600</sub> value was measured. The bile salt tolerance of the strain was calculated using the following formula:

$$\text{Bile Salt Tolerance (\%)} = 1 - (A_n - A_b)/A_n \times 100\%$$

where  $A_n$  represents the OD<sub>600</sub> value at 0% bile salts concentration, and  $A_b$  represents the OD<sub>600</sub> value at 0.3% or 0.5% bile salts concentration.

### 2.7.4. Evaluation of Surface Hydrophobicity

The surface hydrophobicity of the strains was measured using the microbial adhesion to hydrocarbons (MATH) method with minor modifications as per previous methods [24]. Each strain was cultured in MRS medium for 12 h, centrifuged at 5000 g for 10 min at 4 °C, and after washing three times with PBS, the strains were resuspended and the OD<sub>600</sub> value was determined as the initial absorbance ( $A_0$ ). Then, 3 mL of suspension was mixed with 1 mL of xylene as the solvent, vigorously shaken for 15 min, left at room temperature for 1 h, and the lower aqueous phase was collected and measured at OD<sub>600</sub> (A). The surface hydrophobicity of LAB was calculated using the microbial adhesion to hydrocarbons formula:

$$\text{Hydrophobicity (\%)} = 1 - (A_0 - A)/A_0 \times 100\%$$

where  $A_0$  is the absorbance value of the initial bacterial suspension, and A is the absorbance value of the aqueous phase after xylene treatment.

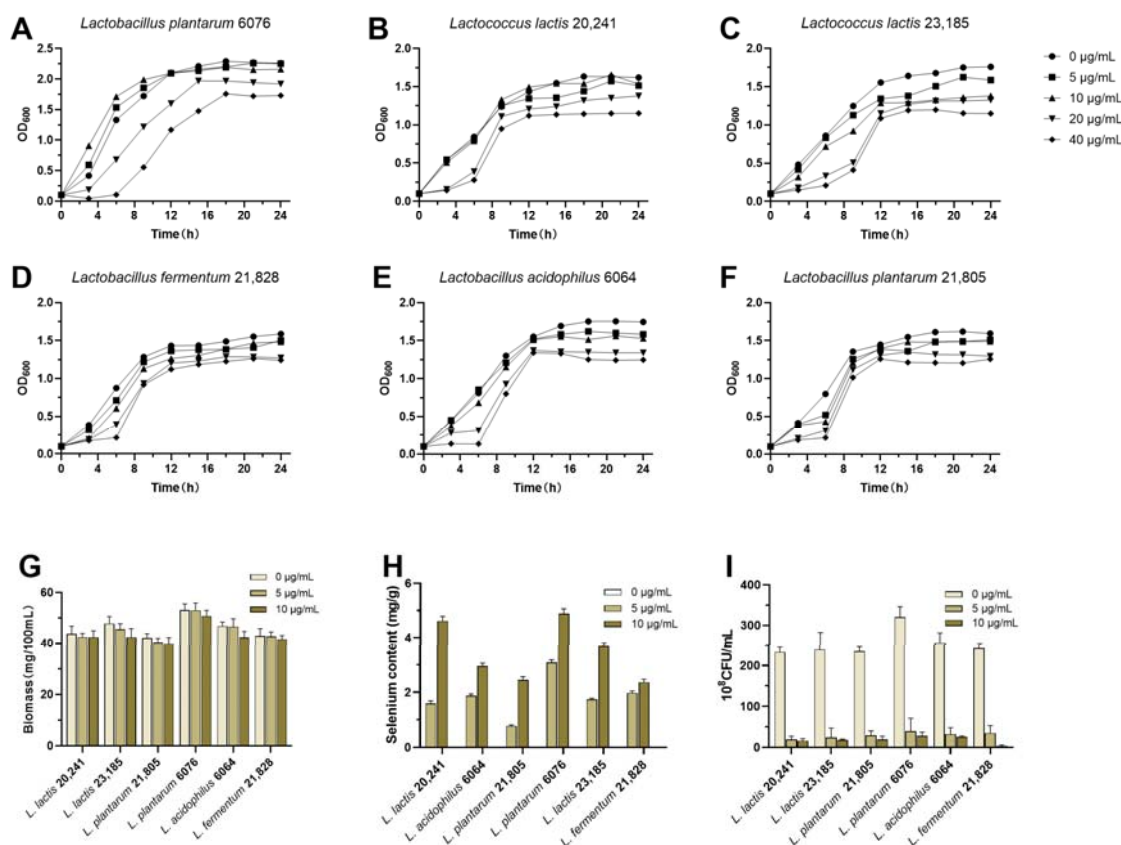
## 2.8. Statistical Analysis

Each experiment was conducted in triplicate. The statistical data are presented as mean ± standard deviation (SD). One-way analyses of variance (ANOVA) with Tukey test were performed using SPSS 10.0 software (SPSS Inc., Chicago, IL, USA). Graphs were generated using GraphPad Prism software 6.01 (GraphPad Software Inc., La Jolla, CA, USA).

### 3. Results

#### 3.1. Screening of Se-Enriched LAB

In this study, six LAB strains were purchased, and Se-enriched strains were obtained by culturing these LAB in MRS medium with different concentrations of sodium selenite for three generations. Figure 1 depicts the influence of Se concentrations on the growth of six LAB. Growth curves of LAB were obtained under Se concentrations ranging from 0 to 40 µg/mL, as shown in Figure 1A–F. It was observed that increasing Se concentrations had a retarding and inhibiting effect on LAB growth. At Se concentrations of 0–10 µg/mL, the optical density (OD) value was relatively high. After 3 h of incubation, bacterial cultures entered the logarithmic growth phase and stabilized around 12 h. However, at Se concentrations of 20–40 µg/mL, the OD value decreased. During the initial 0–6 h, there was a lag in bacterial growth, but after 6 h, bacterial cultures entered the logarithmic growth phase, with the stabilization period extending to 16 h, and the bacterial growth was inhibited to varying degrees. Therefore, Se cultivation concentrations of 0, 5, and 10 µg/mL were selected during the Se enrichment process, and the fermentation time was extended to 18 h for the screening of Se-enriched strains based on biomass, viable bacterial count, and Se content.



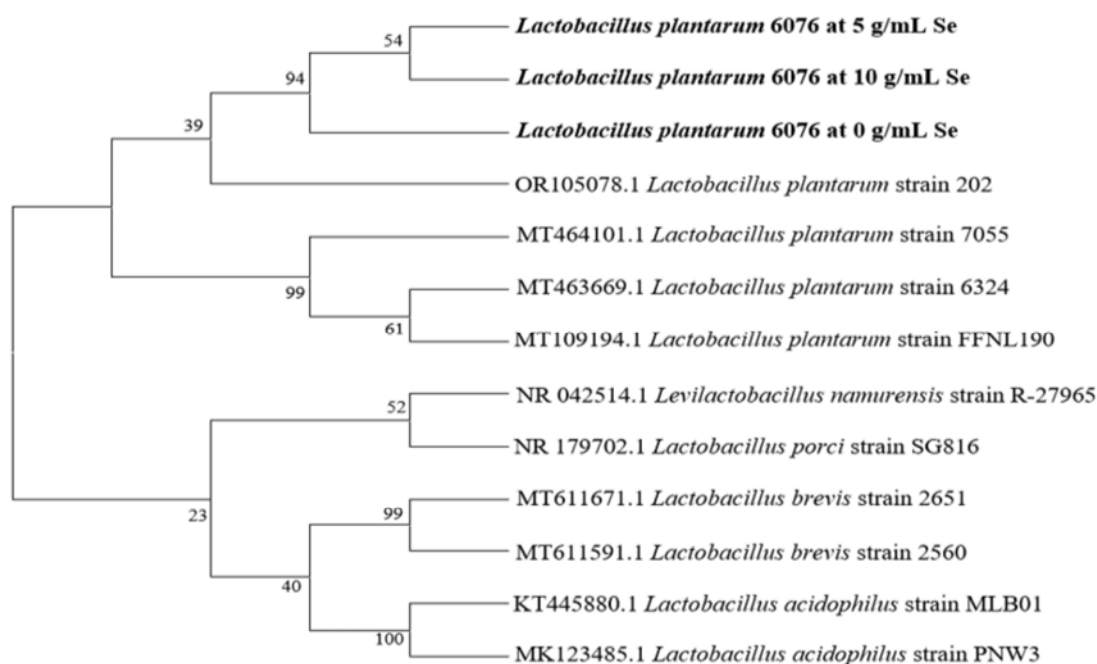
**Figure 1.** Effect of Se concentrations on the growth of lactic acid bacteria. (A–F) Growth curves of strains at 0, 5, 10, 20, 40 µg/mL Se; (G) biomass at 0, 5, 10 µg/mL Se; (H) Se content at 0, 5, 10 µg/mL Se; (I) viable bacterial count at 0, 5, 10 µg/mL Se.

Figure 1G illustrates the variation in biomass of the six strains at Se concentrations of 0, 5, and 10 µg/mL. It was observed that as the Se concentration increased, the biomass of the bacteria decreased. Under Se-free conditions, the strains exhibited the following biomass order: *L. plantarum* 6076 > *L. lactis* 23,185 > *L. acidophilus* 6064 > *L. lactis* 20,241 > *L. fermentum* 21,828 > *L. plantarum* 21,805. At a Se concentration of 10 µg/mL, the strains exhibited the following biomass order: *L. plantarum* 6076 > *L. lactis* 23,185 > *L. lactis* 20,241 > *L. plantarum* 21,805 > *L. acidophilus* 6064 > *L. fermentum* 21,828.

In Figure 1H, a strong positive correlation between bacterial Se content and Se concentration in the culture medium is demonstrated. These strains exhibited the ability to absorb selenite when cultured in MRS medium containing 5 and 10 µg/mL Se. Under the condition of 10 µg/mL Se, *L. plantarum* 6076 and *L. lactis* 23,185 exhibited higher Se accumulation, reaching  $4.88 \pm 0.39$  mg/g and  $3.68 \pm 0.23$  mg/g, respectively. Figure 1I revealed that as the Se concentration increased, the viable bacterial count of the strains decreased. *L. plantarum* 6076 displayed strong Se tolerance, with a viable bacterial count of  $3.9 \times 10^{10}$  and  $2.8 \times 10^{10}$  CFU/mL after 18 h of cultivation in 5 and 10 µg/mL Se, respectively. Based on biomass, viable cell count, and Se enrichment, *L. plantarum* 6076 exhibited a positive correlation and excelled in all three aspects, thus establishing it as the preferred strain for Se enrichment.

### 3.2. Phylogenetic Analysis of Se-Enriched *L. plantarum*

The identification of Se-enriched *L. plantarum* 6076 was conducted through analysis of 16S rRNA sequences. Phylogenetic clustering analysis, as depicted in Figure 2, revealed a 97% sequence homology between *L. plantarum* 6076 and *L. plantarum* 202 (OR105078.1). The gene homology of *L. plantarum* 6076 at 5 µg/mL Se and *L. plantarum* FNL190 (MT109194.1) was determined to be 99%. Moreover, *L. plantarum* at 10 µg/mL Se exhibited a 99.93% homology with *L. plantarum* 7055 (MT464101.1). Consequently, it was established that *L. plantarum* 6076 at 5, 10 µg/mL Se belonged to the *L. plantarum* species.



**Figure 2.** Phylogenetic tree of *L. plantarum* 6076 at 0, 5, 10 µg/mL Se. The bold represents the tested strains.

### 3.3. Structural Characterization of Se-Enriched *L. plantarum*

To investigate the impact of Se on *L. plantarum* 6076, SEM was employed to observe the morphology changes in *L. plantarum* 6076 cultured at different Se concentrations (Figure 3). Under 0 µg/mL Se, *L. plantarum* 6076 exhibited an intact cell morphology, appearing as short rods with a length of approximately 1–2 µm (Figure 3A). At the lower Se concentration (5 µg/mL), *L. plantarum* 6076 did not show significant changes in cell morphology, but SEM analysis revealed the presence of deposits around the strain wall, indicating potential alterations in the cell surface structure (Figure 3B). Interestingly, at the higher Se concentration (10 µg/mL), *L. plantarum* 6076 did not undergo significant changes in overall cell morphology. However, detailed SEM imaging of the strain surface revealed the presence of

concavities and an increase in surface deposits, suggesting potential modifications in the cell surface topography and composition (Figure 3C).

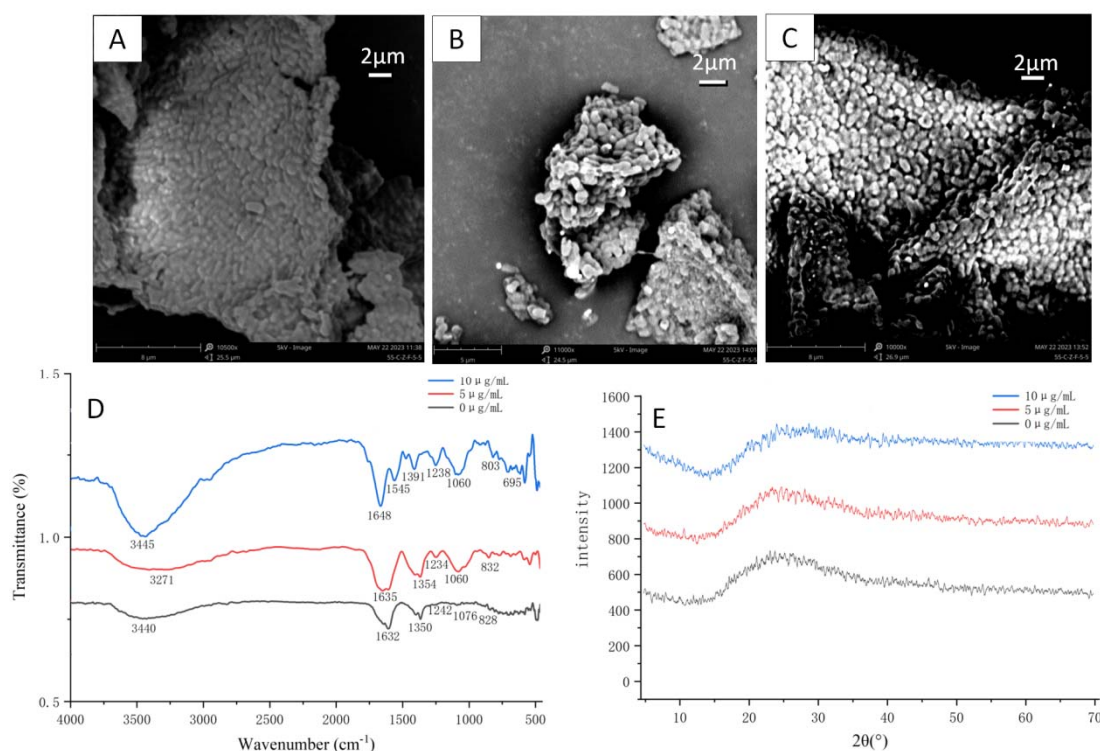


**Figure 3.** Structural characterization of *L. plantarum* 6076 at 0, 5, 10 µg/mL Se. (A) SEM images of *L. plantarum* 6076 at 0 µg/mL Se. (B) SEM image of *L. plantarum* 6076 at 5 µg/mL Se. (C) SEM image of *L. plantarum* 6076 at 10 µg/mL Se. (D) FT-IR spectra of *L. plantarum* 6076 at 0, 5, 10 µg/mL Se. (E) XRD spectra of *L. plantarum* 6076 at 0, 5, 10 µg/mL Se.

To investigate the influence of Se on the functional groups of *L. plantarum* 6076, FT-IR was employed to assess the changes in the functional groups of *L. plantarum* 6076 at 0, 5, 10 µg/mL Se (Figure 3D). The overall waveform of the three samples exhibited similarities, with noticeable shifts in some peak positions. Absorption peaks were detected at 3271–3445 cm<sup>-1</sup>, 1350–1391 cm<sup>-1</sup>, 1234–1242 cm<sup>-1</sup>, 1060–1076 cm<sup>-1</sup>, 803–828 cm<sup>-1</sup>, which became more pronounced and intensified with increasing Se cultivation concentration. In contrast to *L. plantarum* 6076 at 0 and 5 µg/mL Se, *L. plantarum* 6076 at 10 µg/mL Se concentration displayed distinct absorption peaks at 1545 cm<sup>-1</sup> and 695 cm<sup>-1</sup>. XRD analysis revealed consistent spectrum lines for *L. plantarum* 6076 at 0, 5, 10 µg/mL Se across the entire scanning angle range, with broad diffraction peaks observed at 2θ angles ranging from 15° to 35° (Figure 3E).

### 3.4. Probiotic Characteristics of Se-Enriched *L. plantarum*

The probiotic characteristics of Se-enriched *L. plantarum* 6076 were assessed as depicted in Figure 4. *L. plantarum* 6076 at 0, 5, 10 µg/mL Se was inoculated into a simulated gastrointestinal environment, and viable counts were measured to calculate survival rates and tolerance to simulated gastrointestinal conditions. After *L. plantarum* 6076 entered the gastrointestinal environment, the number of viable bacteria gradually declined over time with a relatively stable downward trend (Figure 4A). In the gastric juice, the survival rates for *L. plantarum* 6076 at 0, 5, 10 µg/mL Se were 81.32% ± 5.11, 74.04% ± 2.53 and 70.39% ± 3.7, respectively. In the intestinal fluid, the survival rates were 45.53% ± 3.17, 40.58% ± 1.82 and 37.04% ± 3.25, respectively.

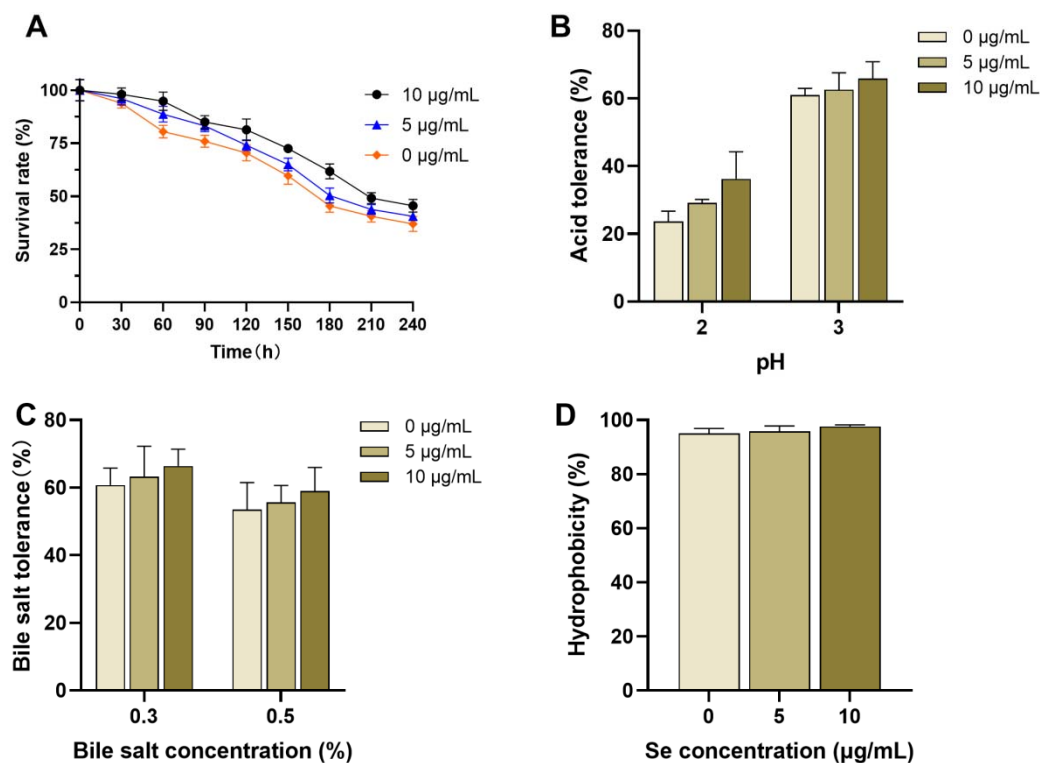


**Figure 4.** Probiotic attributes of *L. plantarum* 6076 at 0, 5, 10 µg/mL Se. (A) Viability in simulated gastrointestinal fluid (tolerance to simulated gastric fluid for 0–120 min; tolerance to simulated intestinal fluid for 120–240 min). (B) Acid resistance. (C) Bile salt tolerance. (D) Hydrophobicity.

The acid tolerance of Se-enriched *L. plantarum* was evaluated by subjecting the strains to incubation under strong acidic conditions at pH 2 and pH 3 for 5 h (Figure 4B). As acidity increased, the survival rates of strains notably decreased. At a pH of 3, all strains displayed elevated survival rates, with *L. plantarum* 6076 exhibiting the highest rate at 10 µg/mL Se concentration, reaching  $65.82\% \pm 4.18$ , followed by *L. plantarum* 6076 at 5 µg/mL Se with  $62.55\% \pm 4.36$ . However, at a pH of 2, the survival rates significantly decreased for all strains. *L. plantarum* 6076 at Se concentrations of 0, 5, and 10 µg/mL had survival rates of  $23.73\% \pm 3.25$ ,  $29.15\% \pm 1.41$ , and  $36.23\% \pm 6.15$ , respectively. Remarkably, the Se-enriched *L. plantarum* 6076 demonstrated greater tolerance compared to *L. plantarum* 6076 under these acidic conditions. Moreover, an increase in Se concentration correlated with an improved acid tolerance of Se-enriched *L. plantarum*.

Bile tolerance is one of the fundamental criteria for evaluating probiotics. Se-enriched *L. plantarum* exhibited varying degrees of tolerance at bile salt concentrations of 0.3% and 0.5% (Figure 4C). At a 0.3% bile concentration, *L. plantarum* 6076 at 10 µg/mL Se displayed the highest bile tolerance, with a survival rate of  $66.37\% \pm 3.83$ , followed by *L. plantarum* 6076 at 5 µg/mL Se with a survival rate of  $63.24\% \pm 7.66$ . At 0.5% bile concentration, the survival rate of *L. plantarum* 6076 at 10 µg/mL Se was  $58.96\% \pm 5.45$ , while *L. plantarum* 6076 at 5 and 0 µg/mL Se had survival rates of  $55.64\% \pm 4.38$  and  $53.55\% \pm 6.27$ , respectively. The ability of bacteria to adhere to different hydrocarbons serves as an important indicator of their hydrophobicity. As illustrated in Figure 4D, *L. plantarum* 6076 at 0, 5, 10 µg/mL Se exhibited strong hydrophobicity, with average adhesion values of  $97.66\% \pm 0.53$ ,  $95.89\% \pm 1.99$ , and  $95.04\% \pm 2.83$ , respectively.

#### 4. Discussion

This study investigated the effect of Se concentration on the growth and enrichment of LAB, and evaluated the changes in the probiotic characteristics of Se-enriched LAB. The research revealed that high Se concentrations (20–40 µg/mL) have an inhibitory effect on

LAB growth, while at a concentration of 10 µg/mL, LAB maintained their integrity and demonstrated Se enrichment capability. Furthermore, LAB exhibit enhanced probiotic properties, suggesting that Se-enriched LAB may offer superior health benefits compared to traditional LAB strains and could be utilized in the development of new probiotic products with enhanced functionality.

The tolerance of LAB to different Se concentrations varies depending on the strain used [25]. Thus, the study observed the influence of different Se concentrations (0, 5, 10, 20, 40 µg/mL) on the growth of six LAB strains. The findings indicated that the LAB were able to grow normally at Se concentrations of 5 and 10 µg/mL, while their growth was inhibited at higher Se concentrations of 20–40 µg/mL. Similar patterns of Se tolerance have also been observed in studies of *L. reuteri*, *L. animalis*, and *L. casei*, with *L. casei* demonstrating higher Se tolerance compared to other LAB [24,26,27].

Environmental changes can induce genetic mutations in organisms, providing a pathway for biological evolution and the emergence of new species [28]. In Se-rich environments, microorganisms may undergo adaptive genetic variations to cope with environmental changes [29]. Consequently, an assessment of the similarity in 16S rRNA sequences between Se-enriched *L. plantarum* 6076 and *L. plantarum* 6076 was conducted. The findings indicated that the genes of Se-enriched *L. plantarum* did not exhibit significant changes, suggesting that the adaptation of *L. plantarum* 6076 to Se-rich conditions did not lead to significant genetic variation at the gene level. This observation implies that the Se enrichment capacity of *L. plantarum* 6076 in Se-rich environments is achieved through its existing metabolic pathways and genomic characteristics, rather than through new genetic mutations or genetic recombination.

In high-Se environments, microorganisms may experience toxicity, leading to the conversion of inorganic Se into Se nanoparticles by bacteria, which possess the ability to bind Se with extracellular polysaccharides [30]. In this study, we observed slight depressions on the surface morphology of plant lactobacilli as the Se concentration increased, and sedimentation around the cell wall, possibly due to the aggregation of Se nanoparticles or binding with polysaccharides produced by lactic acid. The process of Se transformation may cause changes in microbial morphology and biosynthesis [31], allowing for Se to enter the microbial body and be bound with Se proteins [32], Se nucleic acids [33], and Se polysaccharides [34]. Our FTIR spectra revealed changes in the chemical bonds by shifts in the position or intensity of characteristic peaks. These changes may be due to biosynthesis or metabolic alterations induced by high-Se-concentration environments [35]. This indicates that plant lactobacilli have the capability to uptake Se and bind it with intracellular proteins, polysaccharides, and nucleic acids, thereby affecting the corresponding chemical bonds. Therefore, a Se environment may cause modifications in the cellular structure and chemical composition of microorganisms, which is important for comprehending the adaptability of plant lactobacilli in Se-rich environments and their applications.

Probiotics enriched with nano Se have been demonstrated to enhance immune responses, such as alleviating inflammation, boosting antioxidant function, exerting therapeutic effects on tumors, exhibiting anticancer activity, and regulating the gut microbiota [36]. The findings of this investigation suggest that Se enrichment enhances the probiotic properties of *L. plantarum*. Similarly, in comparison to *L. brevis*, Se-rich *L. brevis* displays heightened capacities for scavenging free radicals and reducing agents [37].

## 5. Conclusions

In this study, we screened and characterized dominant Se-enriched LAB and evaluated their probiotic properties. High Se concentrations (20–40 µg/mL) had an inhibitory effect on the growth of the LAB strain. However, LAB exhibited a high Se enrichment ability at a Se concentration of 10 µg/mL, with Se accumulating in an amorphous or non-crystalline form. Furthermore, Se enrichment enhanced the probiotic properties of LAB. Therefore, Se-enriched LAB have the potential to be developed as a functional food or dietary supplement for human and animal consumption.

**Author Contributions:** Methodology, software, validation, L.Z., Z.C., X.Z. and B.Z.; formal analysis, investigation, resources, data curation, A.L. and W.Z.; writing—original draft preparation, L.Z.; writing—review and editing, funding acquisition, T.Y.; visualization, supervision, project administration, Y.Y. All authors have read and agreed to the published version of the manuscript.

**Funding:** This research was funded by [Science and Technology Department of Shaanxi Province] grant number [2022NY-041], [“Co-construction of City and School” scientific research project of State Key Laboratory of Qinba Biological Resources and Ecological Environment (Cultivation)] grant number [SXC-2112], and [Collaborative Innovation Center project of Shaanxi Education Department] grant number [21JY007].

**Institutional Review Board Statement:** Not applicable.

**Informed Consent Statement:** Not applicable.

**Data Availability Statement:** The data are available from the authors on reasonable request.

**Acknowledgments:** We would like to express our gratitude to the team members of the Health Food Manufacturing and Safety Laboratory for their assistance, and Science and Technology Department of Shaanxi Province [2023-JC-YB-404].

**Conflicts of Interest:** The authors confirm that they have no conflict of interest with respect to the work described in this manuscript.

## References

1. Pecoraro, B.M.; Leal, D.F.; Frias-De-Diego, A.; Browning, M.; Odle, J.; Crisci, E. The health benefits of selenium in food animals: A review. *J. Anim. Sci. Biotechnol.* **2022**, *13*, 58. [[CrossRef](#)] [[PubMed](#)]
2. Rayman, M.P. The importance of selenium to human health. *Lancet* **2000**, *356*, 233–241. [[CrossRef](#)] [[PubMed](#)]
3. Wang, B.; Zhao, N.; Li, J.; Xu, R.; Wang, T.; Guo, L.; Ma, M.; Fan, M.; Wei, X. Selenium-enriched *Lactobacillus plantarum* improves the antioxidant activity and flavor properties of fermented *Pleurotus eryngii*. *Food Chem.* **2021**, *345*, 128770. [[CrossRef](#)] [[PubMed](#)]
4. Chao, W.; Rao, S.; Chen, Q.; Zhang, W.; Liao, Y.; Ye, J.; Cheng, S.; Yang, X.; Xu, F. Advances in Research on the Involvement of Selenium in Regulating Plant Ecosystems. *Plants* **2022**, *11*, 2712. [[CrossRef](#)] [[PubMed](#)]
5. Zhang, H.; Qiu, H.; Wang, S.; Zhang, Y. Association of habitually low intake of dietary selenium with new-onset stroke: A retrospective cohort study (2004–2015 China Health and Nutrition Survey). *Front. Public Health* **2022**, *10*, 1115908. [[CrossRef](#)]
6. Zhang, Z.; Lv, J.; Pan, L.; Zhang, Y. Roles and applications of probiotic *Lactobacillus* strains. *Appl. Microbiol. Biotechnol.* **2018**, *102*, 8135–8143. [[CrossRef](#)]
7. Abid, R.; Waseem, H.; Ali, J.; Ghazanfar, S.; Muhammad Ali, G.; Elsbali, A.M.; Alharethi, S.H. Probiotic Yeast *Saccharomyces*: Back to Nature to Improve Human Health. *J. Fungi* **2022**, *8*, 444. [[CrossRef](#)]
8. Staniszewski, A.; Kordowska-Wiater, M. Probiotic and Potentially Probiotic Yeasts-Characteristics and Food Application. *Foods* **2021**, *10*, 1306. [[CrossRef](#)]
9. Fenster, K.; Freeburg, B.; Hollard, C.; Wong, C.; Rønhave Laursen, R.; Ouwehand, A.C. The Production and Delivery of Probiotics: A Review of a Practical Approach. *Microorganisms* **2019**, *7*, 83. [[CrossRef](#)]
10. De Filippis, F.; Pasolli, E.; Ercolini, D. The food-gut axis: Lactic acid bacteria and their link to food, the gut microbiome and human health. *FEMS Microbiol. Rev.* **2020**, *44*, 454–489. [[CrossRef](#)]
11. Ma, C.; Guo, H.; Chang, H.; Huang, S.; Jiang, S.; Huo, D.; Zhang, J.; Zhu, X. The effects of exopolysaccharides and exopolysaccharide-producing *Lactobacillus* on the intestinal microbiome of zebrafish (*Danio rerio*). *BMC Microbiol.* **2020**, *20*, 300. [[CrossRef](#)]
12. Morita, Y.; Jounai, K.; Miyake, M.; Inaba, M.; Kanauchi, O. Effect of Heat-Killed *Lactobacillus paracasei* KW3110 Ingestion on Ocular Disorders Caused by Visual Display Terminal (VDT) Loads: A Randomized, Double-Blind, Placebo-Controlled Parallel-Group Study. *Nutrients* **2018**, *10*, 1058. [[CrossRef](#)]
13. Wan, B.; Wei, L.J.; Tan, T.M.; Qin, L.; Wang, H. Inhibitory effect and mechanism of *Lactobacillus crispatus* on cervical precancerous cells Ect1/E6E7 and screening of early warning factors. *Infect. Agents Cancer* **2023**, *18*, 5. [[CrossRef](#)] [[PubMed](#)]
14. Pophaly, S.D.; Poonam; Singh, P.; Kumar, H.; Tomar, S.K.; Singh, R. Selenium enrichment of lactic acid bacteria and bifidobacteria: A functional food perspective. *Trends Food Sci. Technol.* **2014**, *39*, 135–145. [[CrossRef](#)]
15. Yang, J.; Wang, J.; Yang, K.; Liu, M.; Qi, Y.; Zhang, T.; Fan, M.; Wei, X. Antibacterial activity of selenium-enriched lactic acid bacteria against common food-borne pathogens in vitro. *J. Dairy Sci.* **2018**, *101*, 1930–1942. [[CrossRef](#)] [[PubMed](#)]
16. Mörschbacher, A.P.; Dullius, A.; Dullius, C.H.; Bandt, C.R.; Kuhn, D.; Brietzke, D.T.; José Malmann Kuffel, F.; Etgeton, H.P.; Altmayer, T.; Gonçalves, T.E.; et al. Assessment of selenium bioaccumulation in lactic acid bacteria. *J. Dairy Sci.* **2018**, *101*, 10626–10635. [[CrossRef](#)] [[PubMed](#)]
17. Wang, M.; Ali, F.; Wang, M.; Dinh, Q.T.; Zhou, F.; Bañuelos, G.S.; Liang, D. Understanding boosting selenium accumulation in Wheat (*Triticum aestivum* L.) following foliar selenium application at different stages, forms, and doses. *Environ. Sci. Pollut. Res.* **2020**, *27*, 717–728. [[CrossRef](#)] [[PubMed](#)]

18. Drancourt, M.; Berger, P.; Raoult, D. Systematic 16S rRNA gene sequencing of atypical clinical isolates identified 27 new bacterial species associated with humans. *J. Clin. Microbiol.* **2004**, *42*, 2197–2202. [[CrossRef](#)] [[PubMed](#)]
19. El-Sayed, E.S.R.; Abdelhakim, H.K.; Ahmed, A.S. Solid-state fermentation for enhanced production of selenium nanoparticles by gamma-irradiated *Monascus purpureus* and their biological evaluation and photocatalytic activities. *Bioprocess. Biosyst. Eng.* **2020**, *43*, 797–809. [[CrossRef](#)]
20. Zan, L.; Wang, C. Mediated by tea polypeptides: A green synthesis approach for selenium nanoparticles exhibiting potent antioxidant and antibacterial properties. *Int. J. Food Prop.* **2023**, *26*, 1797–1814. [[CrossRef](#)]
21. Shu, G.; Mei, S.; Chen, L.; Zhang, B.; Guo, M.; Cui, X.; Chen, H. Screening, identification, and application of selenium-enriched *Lactobacillus* in goat milk powder and tablet. *J. Food Process. Preserv.* **2020**, *44*, e14470. [[CrossRef](#)]
22. Taj, R.; Masud, T.; Sohail, A.; Sammi, S.; Naz, R.; Sharma Khanal, B.K.; Nawaz, M.A. In vitro screening of EPS-producing *Streptococcus thermophilus* strains for their probiotic potential from Dahi. *Food Sci. Nutr.* **2022**, *10*, 2347–2359. [[CrossRef](#)]
23. Kaur, A.; Chopra, K.; Kaur, I.P.; Rishi, P. Salmonella strain specificity determines post-typhoid central nervous system complications: Intervention by *Lactiplantibacillus plantarum* at gut-brain axis. *Front. Microbiol.* **2020**, *11*, 1568. [[CrossRef](#)]
24. Krausova, G.; Kana, A.; Hysrlova, I.; Mrvikova, I.; Kavkova, M. Development of selenized lactic acid bacteria and their selenium bioaccumulation capacity. *Fermentation* **2020**, *6*, 91. [[CrossRef](#)]
25. Hysrlova, I.; Kana, A.; Kantorova, V.; Krausova, G.; Mrvikova, I.; Duskocil, I. Selenium accumulation and biotransformation in *Streptococcus*, *Lactococcus*, and *Enterococcus* strains. *J. Funct. Foods* **2022**, *92*, 105056. [[CrossRef](#)]
26. Sun, Y.; Wang, H.; Zhou, L.; Chang, M.; Yue, T.; Yuan, Y.; Shi, Y. Distribution characteristics of organic selenium in Se-enriched *Lactobacillus (Lactobacillus paracasei)*. *LWT* **2022**, *165*, 113699. [[CrossRef](#)]
27. Martínez, F.G.; Moreno-Martin, G.; Pescuma, M.; Madrid-Albarrán, Y.; Mozzi, F. Biotransformation of Selenium by Lactic Acid Bacteria: Formation of Seleno-Nanoparticles and Seleno-Amino Acids. *Front. Bioeng. Biotechnol.* **2020**, *8*, 506. [[CrossRef](#)]
28. Carja, O.; Liberman, U.; Feldman, M.W. Evolution in changing environments: Modifiers of mutation, recombination, and migration. *Proc. Natl. Acad. Sci. USA* **2014**, *111*, 17935–17940. [[CrossRef](#)]
29. Bera, S.; De Rosa, V.; Rachidi, W.; Diamond, A.M. Does a role for selenium in DNA damage repair explain apparent controversies in its use in chemoprevention? *Mutagenesis* **2013**, *28*, 127–134. [[CrossRef](#)]
30. Pan, D.; Liu, J.; Zeng, X.; Liu, L.; Li, H.; Guo, Y. Immunomodulatory activity of selenium exopolysaccharide produced by *Lactococcus lactis* subsp. *Lactis*. *Food Agric. Immunol.* **2015**, *26*, 248–259. [[CrossRef](#)]
31. Filipovic, M.R.; Zivanovic, J.; Alvarez, B.; Banerjee, R. Chemical Biology of H<sub>2</sub>S Signaling through Persulfidation. *Chem. Rev.* **2018**, *118*, 1253–1337. [[CrossRef](#)]
32. Xu, D.; Yang, L.; Wang, Y.; Wang, G.; Rensing, C.; Zheng, S. Proteins enriched in charged amino acids control the formation and stabilization of selenium nanoparticles in *Comamonas testosteroni* S44. *Sci. Rep.* **2018**, *8*, 4766. [[CrossRef](#)]
33. Farrell, K.M.; Brister, M.M.; Pittelkow, M.; Sølling, T.I.; Crespo-Hernández, C.E. Heavy-Atom-Substituted Nucleobases in Photodynamic Applications: Substitution of Sulfur with Selenium in 6-Thioguanine Induces a Remarkable Increase in the Rate of Triplet Decay in 6-Selenoguanine. *J. Am. Chem. Soc.* **2018**, *140*, 11214–11218. [[CrossRef](#)]
34. Yao, M.; Deng, Y.; Zhao, Z.; Yang, D.; Wan, G.; Xu, X. Selenium Nanoparticles Based on *Morinda officinalis* Polysaccharides: Characterization, Anti-Cancer Activities, and Immune-Enhancing Activities Evaluation In Vitro. *Molecules* **2023**, *28*, 2426. [[CrossRef](#)] [[PubMed](#)]
35. Nie, X.; Yang, X.; He, J.; Liu, P.; Shi, H.; Wang, T.; Zhang, D. Bioconversion of inorganic selenium to less toxic selenium forms by microbes: A review. *Front. Bioeng. Biotechnol.* **2023**, *11*, 1167123. [[CrossRef](#)] [[PubMed](#)]
36. Liu, R.; Sun, W.; Sun, T.; Zhang, W.; Nan, Y.; Zhang, Z.; Xiang, K.; Yang, H.; Wang, F.; Ge, J. Nano selenium-enriched probiotic *Lactobacillus* enhances alum adjuvant activity and promotes antigen-specific systemic and mucosal immunity. *Front. Immunol.* **2023**, *14*, 1116223. [[CrossRef](#)] [[PubMed](#)]
37. Shakibaie, M.; Mohammadi-Khorsand, T.; Adeli-Sardou, M.; Jafari, M.; Amirpour-Rostami, S.; Ameri, A.; Forootanfar, H. Probiotic and antioxidant properties of selenium-enriched *Lactobacillus brevis* LSe isolated from an Iranian traditional dairy product. *J. Trace Elem. Med. Biol.* **2017**, *40*, 1–9. [[CrossRef](#)]

**Disclaimer/Publisher’s Note:** The statements, opinions and data contained in all publications are solely those of the individual author(s) and contributor(s) and not of MDPI and/or the editor(s). MDPI and/or the editor(s) disclaim responsibility for any injury to people or property resulting from any ideas, methods, instructions or products referred to in the content.